Department of Physics
Divison of Particle and Nuclear Physics

Single-Neutron Photo-Nuclear Events for LDMX HCal Calibration

30hp Masters's Thesis, PHYM01

Supervisors:
Ruth Pöttgen
Luis Sarmiento Pico

Co-Supervisor:
Lene Kristian Bryngemark

Author:
Daniel Sahlberg

Presented 5th of June 2025
Academic year 2024/2025

Abstract

The upcoming Light Dark Matter eXperiment (LDMX) aims to push new frontiers in the search for the nature of dark matter. Its electromagnetic calorimeter (ECal) can be calibrated directly from the electron beam in the experiment, however the hadronic calorimeter (HCal) will be installed behind and to the sides of the ECal. Thus, it cannot be calibrated directly and has to be done so through other means. The HCal acts as a veto device and calibration is important for ruling out uninteresting events. Additionally, if dark matter decays into luminous matter within the detectors, accurate energy measurements of their decay products are of great interest to determining the properties of dark matter. In this thesis, we investigate the feasibility of one alternative HCal calibration technique: namely the use of single-neutron photo-nuclear events. The idea is that the incident electrons radiate a single bremsstrahlung photon which in turn kicks out a single neutron in a photo-nuclear interaction in the ECal. Naïvely, one could assume that the missing energy of the electron, the energy of the photon and the kinetic energy of the neutron correlate linearly. We simulate 10^6 such events with GEANT4 and investigate the relations between photon energy, neutron energy, detected ECal energy and detected HCal energy. We find that a fraction of these events can be selected to provide well-defined linear relations between all these quantities while maintaining sufficient statistics for aiding the calibration of the HCal.

Abstrakt

Det kommande Light Dark Matter eXperiment (LDMX) ämnar bryta ny mark i sökandet efter mörk materias natur. Dess elektromagnetiska kalorimeter (ECal) kan kalibreras direkt av elektronstrålen i experimentet, dock så kommer den hadroniska kalorimeteren (HCal) installeras bakom och på sidorna av ECal:en. Den kan därför inte kalibreras direkt och måste göras så genom andra men. HCal:en agerar som en veto-enhet och kalibrering är viktigt för att rensa bort ointressanta event. Om mörk materia sönderfaller till synlig materia, är det dessutom av stort intresse att mäta energin hos sönderfalls-produkterna exakt för att finna egenskaper hos mörk materia. I detta examens-arbete undersöker vi möjligheten hos en alternativ kalibrerings-metod: nämligen användningen av enkel-neutron foto-nukleära event. Idén är att de inkommande elektronerna avger en enkel foton som i sin tur kickar ut en enkel neutron i en foto-nukleär interaktion i ECal:en. Man kan naïvt anta att den avsaknade energin hos elektronen, energin hos fotonen och den kinetiska energin hos neutronen förhåller sig till varandra linjärt. Vi simulerar 10^6 sådana event med GEANT4 och undersöker sambanden mellan foton-energin, neutron-energin, den uppmätta ECal energin och den uppmätta HCal energin. Vi finner att en delmängd av dessa event kan urskiljas som förser väldefinierade linjära samband mellan dessa storheter samtidigt som nog med data behålls för att hjälpa till med kalibreringen av HCal:en.

Acronyms

DM: Dark Matter
GEANT4: Geometry And Tracking (version) 4
ECal: Electromagnetic Calorimeter
HCal: Hadronic Calorimeter
LDM: Light Dark Matter
LDMX: Light Dark Matter eXperiment
SM: Standard Model
WIMP: Weakly-Interacting Massive Particle

Summary

Astronomers discovered in the 1970's that there was not enough matter in the universe to explain certain cosmological phenomena. Modern estimates suggest there would need to be about 6 times as much matter as we could see. As this mysterious extra matter was invisible to us, they named it "dark matter" and the nature of what it is, how it works and where it came from is one of the most pressing questions in modern astrophysics and particle physics. Many experiments have since been designed to search for new particles that could account for dark matter, but to this day none have managed to pin it down. The latest in line for this undertaking will be the Light Dark Matter eXperiment (LDMX) at SLAC near Stanford, USA, which is scheduled for operation in a few years. The premise of LDMX is to send electrons with a known energy towards a target where they interact to hopefully produce dark matter. The leftover energy of the electron and other by-products is measured behind the target by several particle detectors. Since the dark matter particle cannot be detected, any energy is missing from the measurements could indicate production of dark matter.

Like with most measurement devices, the particle detectors must be calibrated to translate their electrical signals to particle energies. This is usually done by sending particles of a known energy into the detectors and characterize their response. For the detectors that are not directly in line-of-sight with the particle beam, this is pretty much impossible. In this thesis, we investigate one possible way to circumvent this issue. There is a series of particle interactions in which the incident electron produces a photon, and this photon kicks out a neutron from a nucleus in the experiment, that occurs relatively frequently. One could hope that the missing energy from the electron corresponds to the energy of the photon, which in turn corresponds to the energy of the neutron. Thus, by measuring the electron energy in the first detector (which is calibrated), one can infer what energy should be measured from the neutron in the second detector. In this thesis, we simulate one million such events to see if these relations hold and how consistently the detectors measure the energies of the particles.

Our results show that there is indeed a good correspondence between missing electron energy, photon energy, neutron energy and detector responses. Additionally, we find that there may be sufficient data over a wide enough energy range to calibrate the HCal well and achieve good energy resolution. However, previous work suggest that this sentiment may not hold between different simulation models, so more work is needed to assess the accuracy of these results.

Acknowledgements

I want to thank my supervisors Ruth Pöttgen and Luis Sarmiento Pico for being supportive and patient with me during this project. You have given me great support and feedback on the results and their interpretations. Thank you for taking me under your wings.

I want to thank my co-supervisor Lene Kristian Bryngemark for their near endless help in debugging and other IT issues. You have helped me fix more issues than I can count. Thank you for keeping my project on its feet.

I want to thank my fellow Master's and Bachelor's students for assistance in the coding and writing workshops. You have brought me much inspiration for coding and writing during this project. Thank you for being in the same boat as me.

I want to thank my friends for the activities we had outside of working hours. You have allowed me much needed breaks from the dreaded work of writing this report. Thank you for ~~putting up with me ;P~~ always being there for me.

I want to thank my other colleagues at the Lund division of LDMX for miscellaneous assistance with the project. From loaning me an office to work in to organizing the aforementioned workshops to fixing some gnarly IT issues. Thank you for making this project possible.

Contents

Chapter 1

Introduction

The nature of dark matter (DM) has been an elusive mystery since its discovery in the 1930's [1]. Many theories and models have been proposed in an attempt to explain what dark matter is, what mass a dark matter particle would have as well as with what interaction strength it interacts with visible matter. Several experiments have also been carried out to probe high particle masses (GeV-TeV) and a wide interaction strength range, yet to this day we only have null results [2]. The upcoming Light Dark-Matter Experiment (LDMX) utilising the LCLS-II accelerator at SLAC near Stanford, USA [3], aims to explore a slightly lower mass range (MeV-GeV) with missing energy and momentum measurements. The experimental idea is to fire 8 GeV electrons at a fixed thin tungsten target which causes the electron to produce dark matter particles in a "dark bremsstrahlung" process, similar to how photons can be radiated in visible bremsstrahlung. As the dark matter particles cannot be detected like visible particles, an electromagnetic calorimeter (ECal) will be used to measure the missing energy of the electron as well as detect photons from visible bremsstrahlung events and other background events. A hadronic calorimeter (HCal) will also be installed behind and to the sides of the ECal to detect and measure other background events. Additionally the HCal could be used to detect decay products of dark matter particles, in which case reliable energy measurements are necessary.

As particle detectors are custom built for experiments, they need to be calibrated by measuring particles of known energy and translating their readouts to this energy. This, unfortunately, is infeasible for the HCal at LDMX as it will be assembled on-site behind the ECal and cannot be calibrated beforehand. An alternative method is instead to calibrate with events in which the incident electron radiates a photon which undergoes a photo-nuclear reaction in the ECal producing a single neutron. Naïvely, the energy of this neutron should more or less correspond to the energy of the photon and, equivalently, to the missing energy of the electron. One would thus expect a linear relationship between these energies. The main goal of this thesis is to assert to which extent this assumption holds true and how precise and feasible it would be to calibrate the real HCal with photo-nuclear events with single neutrons. To do this, we generate large-statistics samples of such events in the simulation and modelling framework GEANT4 [4] and study the correlation between neutron energy, photon energy and missing electron energy. We simulate electrons with a starting energy of 8 GeV and apply filters to only generate bremsstrahlung photons with an energy over 5 GeV. Additionally we investigate whether it is possible to define an event selection that allows us to find a well-defined relation between neutron and photon energy while still maintaining sufficient statistics for calibration. The main points of this project are thus:

- Determine the relation between missing electron energy, neutron energy and photon energy in single-neutron photo-nuclear events.
- Assess whether this relation is linear and well-defined enough to be suitable for calibration.
- Find an event selection that ensures a well-defined relation between neutron and photon energy while maintaining sufficient statistics for calibration.

Chapter 2

Background

2.1 The Search for Dark Matter

2.1.1 Evidence for Dark Matter

In the 1970's, astronomers measured the distribution of velocities of stars in galaxies as a function of their distance from the galactic centers [1, 5]. Their observations showed that stars were moving faster than what Newton's law of gravity and Kepler's third law of planetary motion could explain. The simplest explanation was that there was more matter in galaxies than could be observed. Throughout the rest of the 1900's and into the early 2000's, more and more evidence for this mysterious matter started to emerge [5]. From gravitational lensing stronger than what visible, or luminous, matter should produce, to disturbances of the cosmic microwave background radiation, to the geometry and expansion of the universe; they all started to pile up evidence that there was some other substance in the universe affecting its surroundings only through gravity.

And this was not a question of an abundance of gas clouds too sparse to cradle star formation, or lone black holes that had licked up the last of their accretion disks; observations required over five times as much "invisible" matter as luminous matter to explain the discrepancy [5]. Such vast quantities of matter would be impossible to miss if it interacted with luminous matter as we know it; whether that be via the strong force, the weak force or electromagnetically. As this mysterious elusive non-luminous matter seemingly only interacts gravitationally with luminous matter, we know it today as dark matter (DM), and uncovering what it is and explain its presence is one of the most pressing questions for particle physics and astrophysics today.

2.1.2 Dark Matter Theories and Frontier

As the nature of DM is still very much a mystery, there exists no shortage of theories and models as to what it could be. In truth, we do not even know if DM consists of particles and forces like the standard model (SM) does, but physicists have nonetheless tried to connect DM to other mysteries in the standard model. One of the most promising connections has been that of DM as weakly-interacting massive particles (WIMPs) to supersymmetry. In short, supersymmetry is a theory that predicts that every particle in the SM has a supersymmetric "partner" particle of opposite spin type [6]. In other words, all fermions have super symmetric boson partners and vice versa. Among many different lingering questions in particle physics, supersymmetry was developed to cancel out divergent contributions to the Higgs boson mass as well as answer why the force of gravity is so much weaker than the other fundamental forces. The supersymmetric partner particles have predicted masses between 100-3000 GeV [7], which, combined with their elusive nature, has made some supersymmetry particles promising candidates as WIMP dark matter. WIMPs are the model of DM particles with masses in the GeV~TeV range, which has already been thoroughly probed in several experiments [2].

Other theories of dark matter connect it to theorized particles with very small masses, in the range of μeV~eV [8, 9, 10]. Yet other theories propose that dark matter consists of ancient primordial black holes or that it is an illusion of our incomplete understanding of gravity. The upcoming Light Dark Matter eXperiment (LDMX) aims to search for dark matter in the MeV~GeV mass range, closer to that of WIMPs. DM in this range is simply called "light" dark matter (LDM) and is part of the theory of a "hidden sector" or "dark sector" [2]. In this theory, dark matter particles χ interact with SM matter through a new, unidentified interaction process. The strength of this interaction, as well as the mass of χ, form a parameter space that has not yet been extensively explored by previous experiments. This parameter space has been illustrated in the LDMX design study and shows where LDMX aims to search for dark matter in terms of these parameters [2], which has been recreated in Fig. 2.1 below.

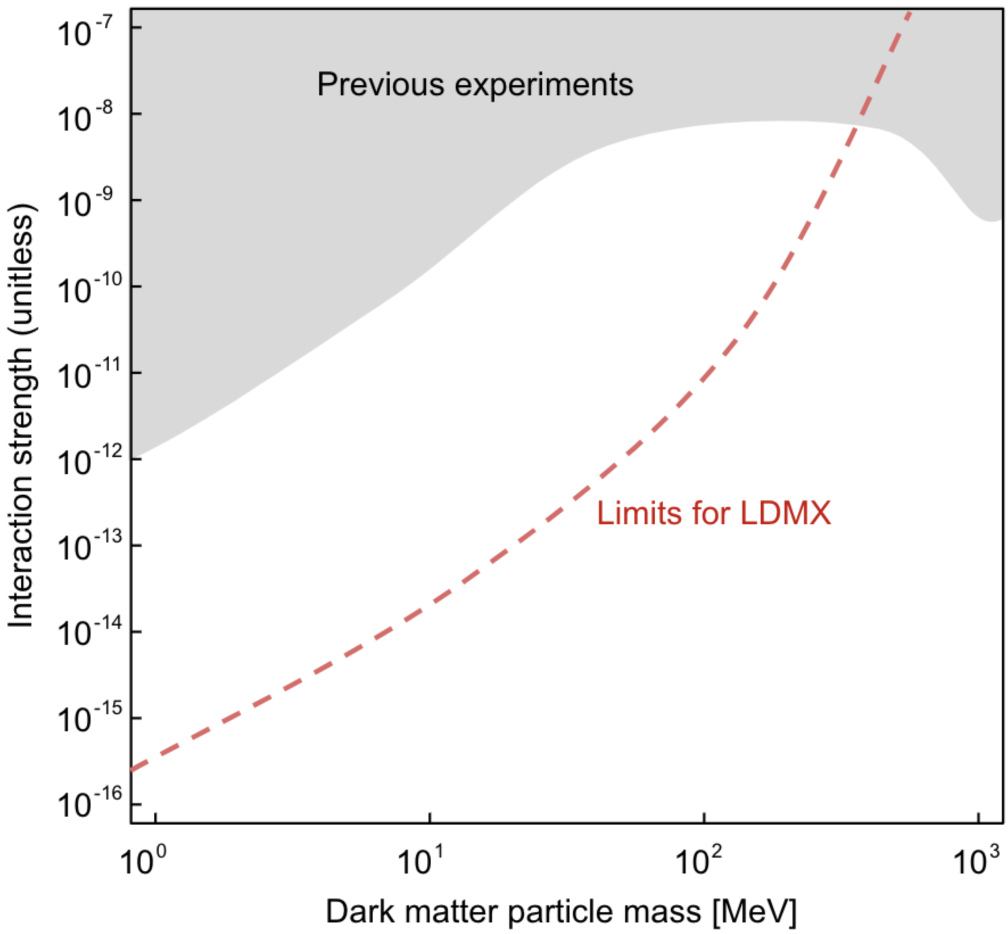

Figure 2.1: Illustration of parameter space for mass and interaction strength of light dark matter. Image inspired by the 2018 LDMX Design Study [2].

2.2 The Light Dark Matter Experiment

2.2.1 Dark Matter Production Process

As previously mentioned, LDMX aims to search for dark matter that is produced by SM particles in a new, unidentified interaction. The setup of the experiment is to use the LCLS-II linear accelerator at SLAC near Stanford, USA, to fire electrons with 8 GeV kinetic energy[1] at a thin target of tungsten [2]. The theory is that as an electron interacts with the target, the electron radiates a dark matter particle and anti-particle pair $\chi + \bar{\chi}$ through a new, unidentified interaction. This interaction process is illustrated in Fig. 2.2 below.

[1]This thesis will use "kinetic energy" and "energy" interchangeably. We will, in all cases, refer to kinetic energy (when applicable) unless specified.

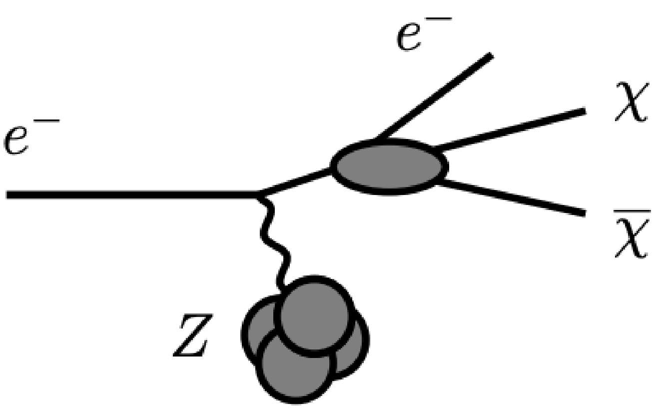

Figure 2.2: Illustration of theorized dark matter production processes. An electron e^- interacts with a nucleus Z and produces a dark matter particle χ and anti-particle $\bar{\chi}$ through an unidentified interaction process. Image credit to the 2018 LDMX Design Study [2].

To identify such an event, the experiment requires an electromagnetic calorimeter (ECal) to detect the recoiling electron and measure its energy. The ECal will be discussed in greater detail in Section 2.2.2. As there are some background processes the ECal cannot detect, a hadronic calorimeter (HCal) will be installed behind and to the sides of the ECal to detect the presence and energies of other particles. The HCal will be discussed in greater detail in Section 2.2.3 and the background processes in Section 2.2.4. Trackers using magnetic fields to measure the momentum of charged particles will also be installed in front of the target and behind the target to measure the particle trajectories outside the calorimeters. Trajectories within the ECal and HCal will be tracked by the trail of energy depositions within each detector, aided by time measurements to differentiate particles with overlapping trajectories. A simple illustration of some of these experimental components and setup can be found in Fig. 2.3, which also shows what signal we expect from a dark matter production event.

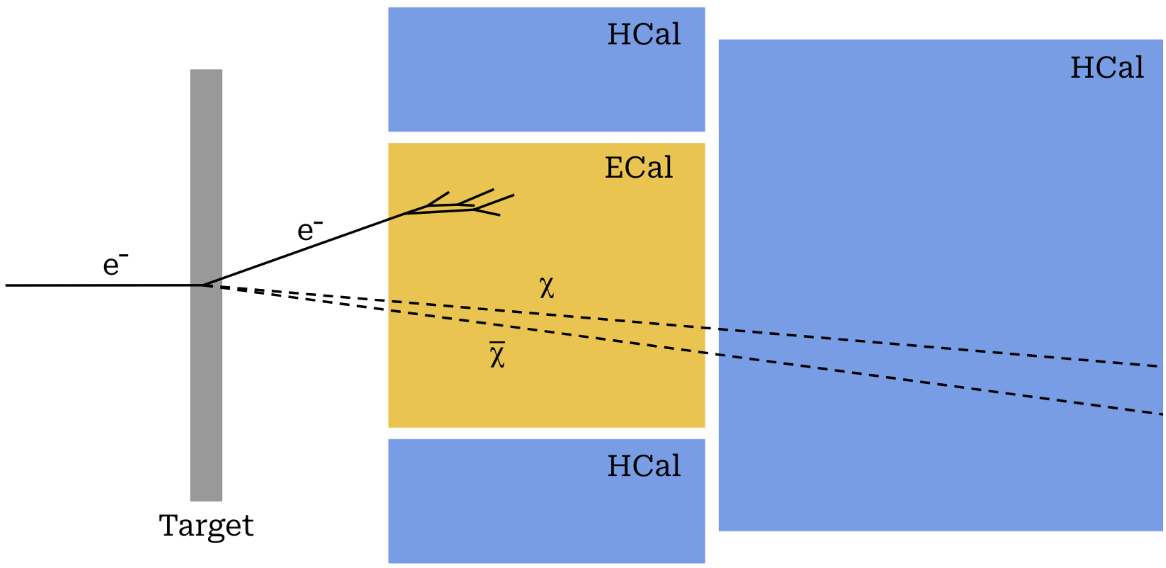

Figure 2.3: Simple illustration of the relevant experimental components and setup of LDMX. An 8 GeV electron beam comes from the left, strikes the target and produces dark matter. The electron is detected in the ECal while the dark matter particles fly straight through both the ECal and the HCal. Figure not to scale.

2.2.2 Electromagnetic Calorimeter

Electromagnetic calorimeters detect and measure particles via electromagnetic interactions [11]. Due to the relativistic velocities of high energy particles and stochastic nature of particle interactions, energies are measured by letting particles deposit their energies across multiple detector layers. In doing so, new particles are often created carrying a part of the parent particle's energy. These may also deposit their energy in the detector layers and create more particles. Due to the potentially vast number of particles generated through these interactions, the collective process is referred to as a "shower", specifically an electromagnetic shower.

The ECal at LDMX will be what is called a sampling calorimeter [2]. In these devices, the layers of measurement units are interspersed by layers of heavy absorbers, which absorb the brunt of particle energies but cannot produce measurements. This allows the ECal to be constructed much more compactly, at the cost of not being able to measure all the particle energies.

While electromagnetic interactions like bremsstrahlung and pair production are particularly prone to occur for electrons, positrons and photons; heavier particles like neutrons, pions and other hadrons may deposit some of their energy in the ECal and start to shower there [12]. Since these showers start deeper in the ECal, or not at all, this is one way to tell hadrons apart from photons and leptons. To capture the full shower of a hadron, however, it is necessary to use a hadronic calorimeter.

2.2.3 Hadronic Calorimeter

Hadronic calorimeters detect and measure particles mainly via strong nuclear interactions [12]. Much like electrons and photons undergo electromagnetic showers in an ECal, hadrons undergo hadronic showers when they pass into an HCal. Due to the multiple quarks and gluons that make up hadrons, hadronic showers can be incredibly varied and complicated, even among the same type of hadrons. Light hadrons may also occasionally radiate photons, which undergo EM showers intertwined with the hadronic shower. These can still be measured by the HCal, although it makes particle identification more difficult.

The HCal at LDMX is, like the ECal, a sampling calorimeter [2]. It is anticipated that it will have poorer energy resolution than the ECal, however it has not yet been calibrated. It is not possible to fully characterize the components before assembly, as the absorbant layers must be taken into account and this can only be done after it has been assembled on-site. It is also not possible to send hadrons with known energies into the HCal, as the LCLS-II accelerator providing electrons is not designed to accelerate hadrons. One alternative method of calibrating the HCal is by using events in which the electron emits a bremsstrahlung photon, which then produces a neutron in a photo-nuclear interaction. The recoil electron's energy can be measured as usual in the calibrated ECal. *If* its missing energy corresponds well to the photon energy and *if* the photon energy corresponds well to the neutron energy, the HCal signal can be calibrated to match the expected neutron energy. In order to make a calibration with enough statistical confidence, there needs to be a sufficient quantity of these events from the incident electrons. This means we must understand the types and rates of background events at LDMX.

2.2.4 Background Events

Researchers at LDMX have already investigated potential background events in the experiment and how to reduce them. Their predictions have been illustrated in the diagram in Fig. 2.4 [13]. The most frequent background process, other than no interaction at all, is bremsstrahlung; where a portion of the electron energy is transferred to a photon. It would result in a second EM shower in the ECal, which is easily identifiable from the lack of trajectory in the trackers. Various other background processes will similarly be reduced by considering particle tracks and energy measurements within the detectors. If dark matter exists within the LDM mass range and it is produced (much) more frequently than the irreducible backgrounds, LDMX aims to find it.

In this project we are primarily interested in photo-nuclear interactions. From the diagram below and other studies, we know that the relative rate of photo-nuclear events is about 10^{-6} to 10^{-5} [2, 13]. From previous work by researchers at LDMX, we know that about 1% of photo-nuclear events would produce a single neutron. For the first pilot run, LDMX anticipates that an integrated electron count on the order of 10^{14} will be delivered to the target [2]. The full run hopes to fire up to 100 times as many electrons, but from the pilot we run can expect around 10^6 single-neutron photo-nuclear events to occur at LDMX. In order to get an idea of how to identify and use them, let us look closer on the interaction in question.

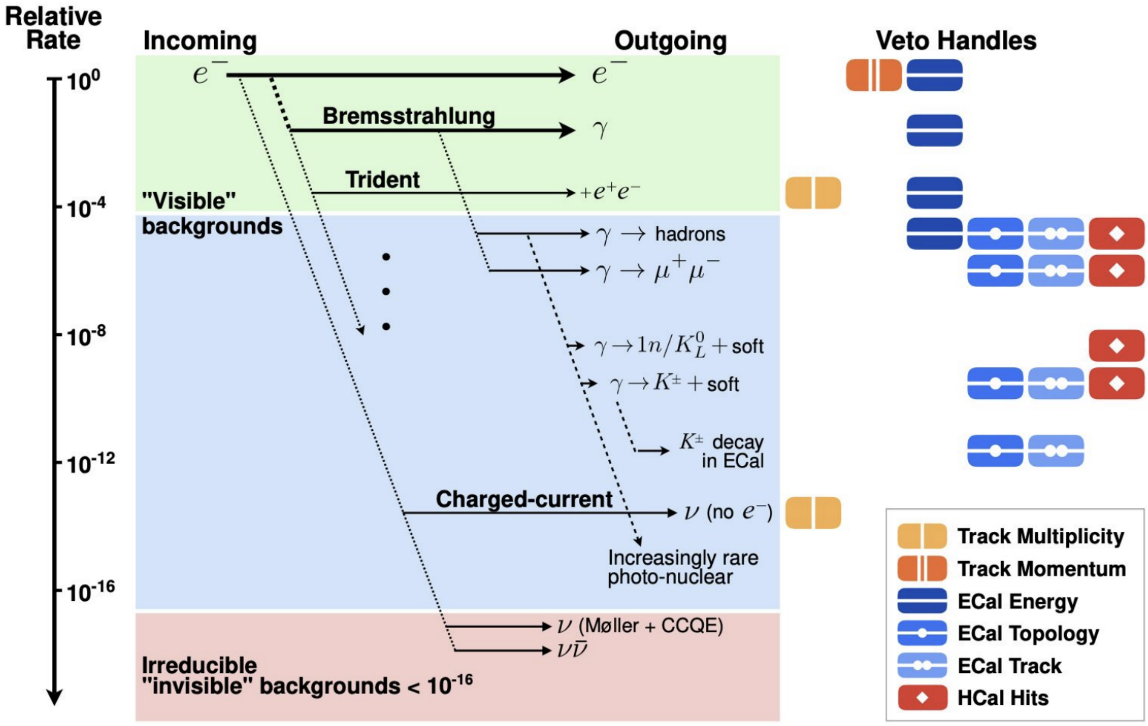

Figure 2.4: Illustration of anticipated background processes at LDMX, their relative rate and what parameters are used to identify and reduce them. Image credit to the 2023 LDMX background rejection investigation [13].

2.3 Photo-Nuclear Interactions

The interactions we focus on in this thesis are single-neutron photo-nuclear events. In these events, the source electron undergoes bremsstrahlung in the target and deposits a portion of its energy in a photon. The electron reaches the ECal and showers as expected, but the photon undergoes a photo-nuclear interaction in the ECal instead of showering. The photon is absorbed by a nucleus in the detector and kicks out a single neutron. The neutron is expected to travel through the ECal without depositing any energy and then showers in the HCal. An illustration of the process can be found in Fig. 2.5. As the missing energy of the electron eludes the ECal, such events could be mistaken for DM signals were it not for the HCal. If the showers can be identified as originating from a single neutron, LDMX could potentially use these events to calibrate the HCal output. The electron energy can be measured by the calibrated ECal, and if its missing energy corresponds to that of the photon, and its energy corresponds to that of the neutron, the HCal signal can be calibrated by what its energy measurements "should" be. How well these energies correlate is one of the questions we aim to answer in this project. In previous work by other researchers at LDMX, simulations of single-neutron photo-nuclear events with photons at an energy of 3 GeV were carried out in four different simulation frameworks, see Fig. 2.6. In the GEANT4 framework [4], most neutrons retained 70 − 80% of the photon energy, while in the FLUKA framework [14], there was no favored retention. In this project we will use the GEANT4 framework to simulate events with photon energies between 5 − 8 GeV and investigate how much energy the neutrons retain as well as how well the detectors measure their energy.

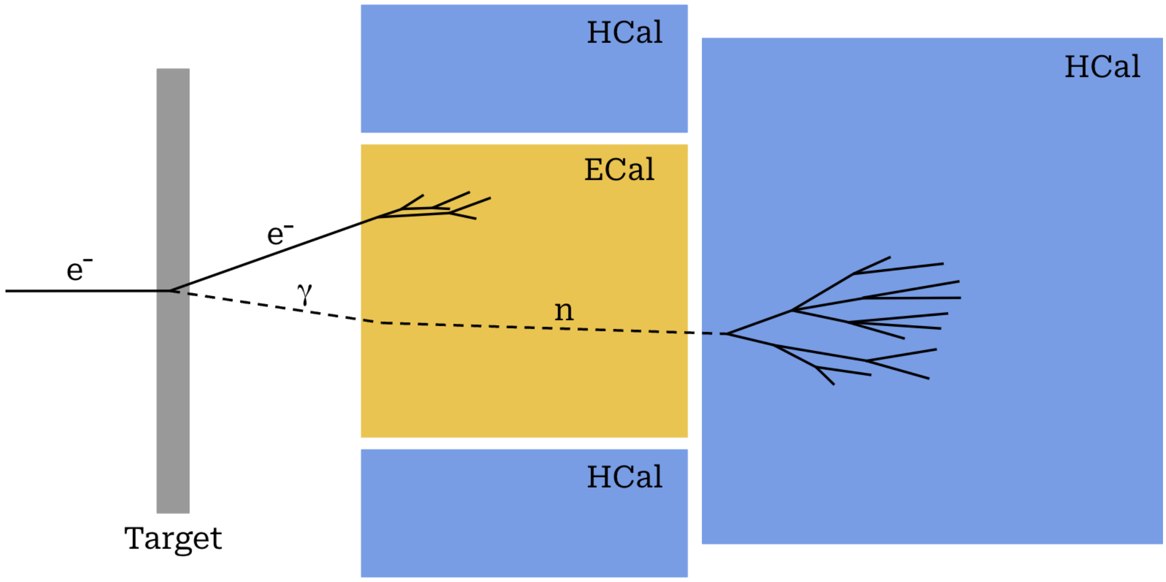

Figure 2.5: Illustration of how a neutron is produced and detected from a photo-nuclear event. Figure not to scale.

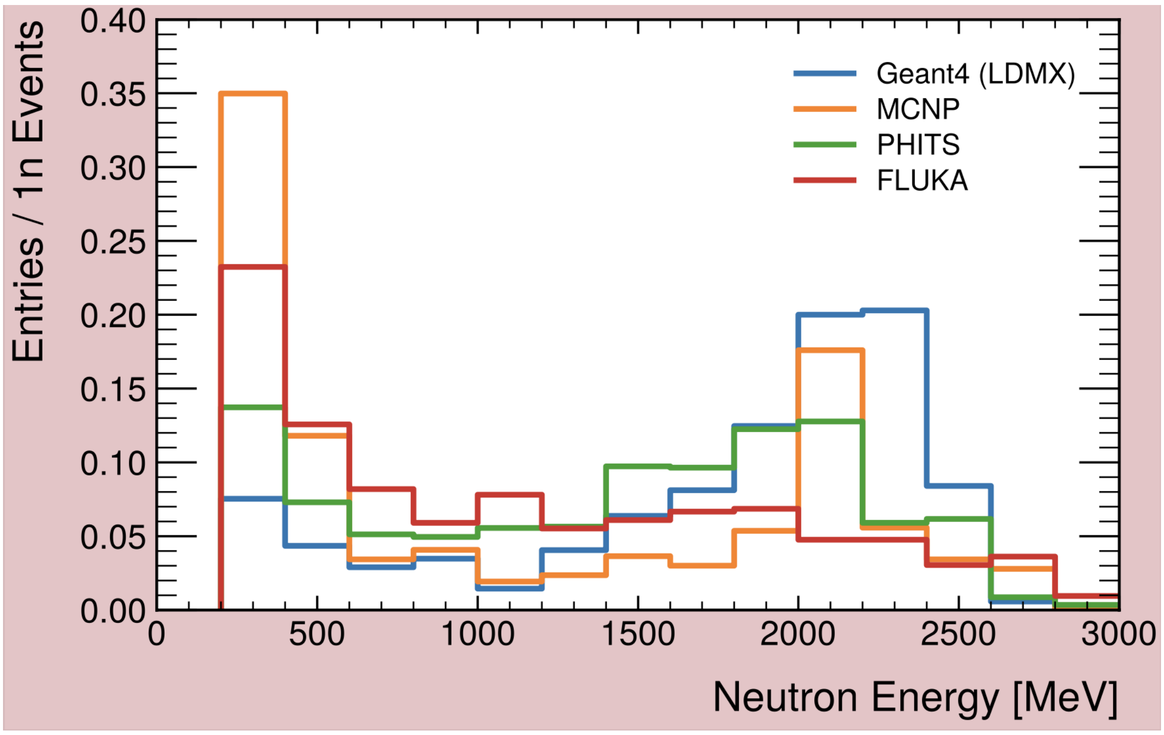

Figure 2.6: Previous single-neutron photo-nuclear interaction simulations where the photon energy was chosen to be 3 GeV. [15]

Chapter 3

Simulation

3.1 Simulation Code and Data Format

The simulation configuration code was taken from previous work by other researchers at LDMX. It was written in Python using ldmx-sw [16] and the general data storage and visualization library ROOT. The ldmx-sw framework makes use of the general particle physics simulation software GEANT4 and allows to specify the experiment and detector setup in full detail. For this thesis, we used the preset detector geometry version `ldmx-det-v14`. The 10^6 electrons were simulated one at a time and generated with the preset `single_8gev_e_upstream_tagger()` generator. The photo-nuclear interaction was modeled with the preset `BertiniSingleNeutronModel()`. As we were only interested in single-neutron photo-nuclear events, we applied biases and filters to the simulation to force only such events. We used a `PhotoNuclear(...)` bias that increased the cross section of photons above 5 GeV to undergo photo-nuclear interactions by 550 times, to improve computation time. We also applied filters to tell the simulation to only save events where the bremsstrahlung photon has an energy over 5 GeV, events where the neutron has a kinetic energy over 200 MeV (this is used to suppress events with multiple neutrons) as well as select events with a single photo-neutron. Since the detectors are simulated as well, their signal output is stored as "reconstructed" data, as opposed to the "real" energy depositions of simulated data. To combat the measurement losses of the absorbing layers, each measurement layer of the ECal is assigned a scaling weight to their signal output. The formula for converting simulated energy depositions to reconstructed energy measurement can be found in Appendix A. The software uses these weights to compensate for how much energy is expected to have been deposited in the previous absorbing layer. The ECal simulation is also outfitted with a veto algorithm using a technique called a boosted decision tree (BDT). The veto is essentially a multivariate algorithm for automatically filtering and discarding events that do not look like potential DM signals. It takes into account parameters such as how large the EM shower is and how much energy is detected outside the shower and summarizes its data as a "discriminator value", which is more or less a measure of how DM signal-like an event is. The complete simulation file is available on GitHub [17].

The simulation results were stored in a .root file as a TTree, which groups related data in "branches" for easier user sorting. For instance, a branch could be ECal detections containing "leaves" of data with position, time of detection or deposited energy. Our interest lied in the `simulated ECal hits`, `reconstructed ECal hits`, `simulated HCal hits`, `reconstructed HCal hits`, `ECal Veto` and `simulated particles` branches. The branches of simulated and reconstructed detector hits contained information about the energy measurements, which was summed for each event to provide a detector response. The simulated ECal hits also contained a leaf storing hit position, which was used to find the layers and layer weights of the hits. The ECal Veto branch contained leaves storing the various parameters it uses to filter events. At first all its parameters were extracted, although during the analysis most were discarded due to turning out uninteresting and to save space. In the end, only a handful were kept. The simulated particles branch contained leaves with information about particles generated in the simulation. It had leaves storing their type, energies, start and end positions, momentum, a list of their daughters and much more. This branch was used to find the bremsstrahlung photon and photo-neutron, which is explained in the next section.

3.2 Event Selection and Analysis Script

To select the relevant events for this project from the vast and detailed simulation data, a custom analyzer was written in C++ based on the documentation tutorial [18]. As there are many particles generated in interactions and showers, ldmx-sw only stores the most relevant particles we specify through the filters and their nearest daughters and parents. All particles are assigned an index upon creation that can be used to check whether the particle was stored in the final output list of particles. Particles are instances of an ldmx-sw class that tracks particle type, energy, momentum, indices of their daughters as well as other parameters. The 8 GeV primary electron always has index 1, so it is trivial to locate and extract its daughters. We loop through its daughters and check the ones that are stored in the final list. If the daughter is a photon with more than 5 GeV energy; we store it as the bremsstrahlung photon. We then loop through this photon's daughters to look for photo-neutrons. Finally, we store the highest energy neutron daughter as the photo-neutron. The complete analysis script is available on GitHub [17].

We also collected various data from the ECal Veto as well as the total energy from all the simulated and reconstructed ECal and HCal hits. As the ECal uses scaling weights to calculate "true" particle energy from deposited energy, we used the layer weights and other constants to calculate a simulated weighted energy in the ECal. These weights and constants were acquired by telling the simulation file to output all its parameters in a JSON file, where we could find the layer weights. In summary, the quantities stored from the simulations were:

- The initial electron energy.
- The photon energy.
- The neutron kinetic energy.
- The discrimination value from the ECal Veto.
- The total weighted simulated energy measurements in the ECal.
- The total reconstructed energy measurements in the ECal.
- The total simulated energy depositions in the HCal.
- The total reconstructed energy measurements in the HCal.

Chapter 4

Analysis

4.1 Energy Ratio and Event Selection

The relation between simulated neutron kinetic energy and photon energy shows a linear relationship, as shown in the 2D histogram in Fig. 4.1. The code for generating all figures in the results is available on GitHub [17]. Most events fall within this linear relation, but the large variance among events is not ideal for calibration. As we want the missing energy of the electron to match the energy of the neutron as close as possible, we equivalently want the energy of the photon to match the energy of the neutron. One could imagine that neutrons that did not deposit their energy in the ECal would be best suited for HCal calibration. These would appear similar to DM signal events in the ECal veto algorithm. An easy way to filter for events with a low variance energy ratio is to examine the parameters of the ECal Veto. As its purpose in the real experiment will be to filter for potential DM signal events, its data will be available to aid selecting photo-nuclear events for calibration. After examining its various parameters and comparing the neutron-photon energy ratio distribution between them, we find that the ECal Veto discriminator value from the BDT shows the lowest variance for events with discriminator value > 0.2, see Fig. 4.2[1].

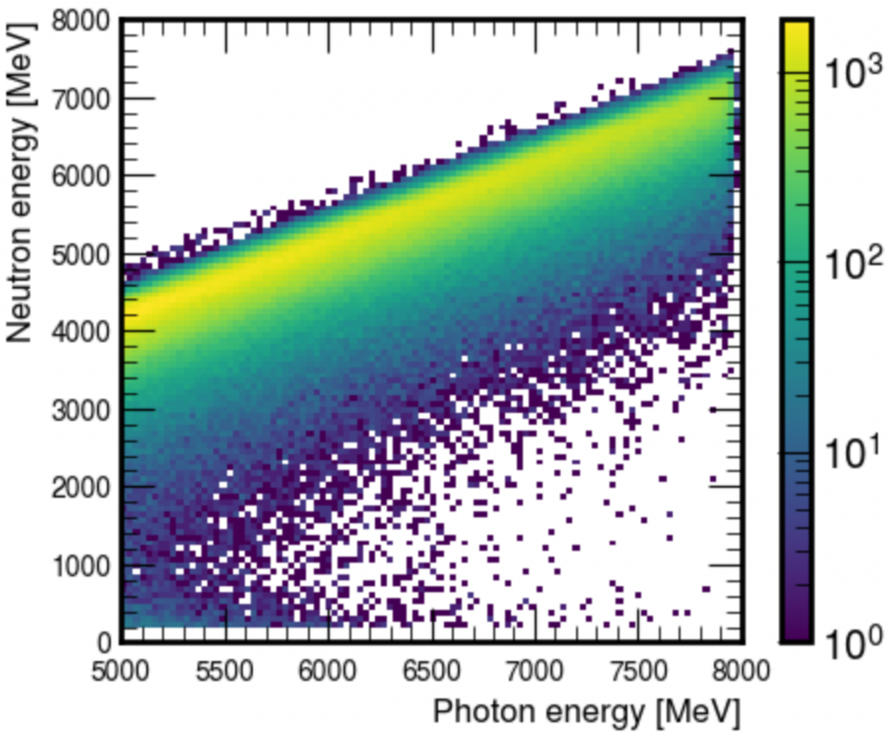

Figure 4.1: The relation between simulated neutron energy and simulated photon energy for 10^6 events.

[1]We examined every available parameter of the ECal Veto, but for the sake of brevity we only display the 6 parameters kept after a debugging hunt.

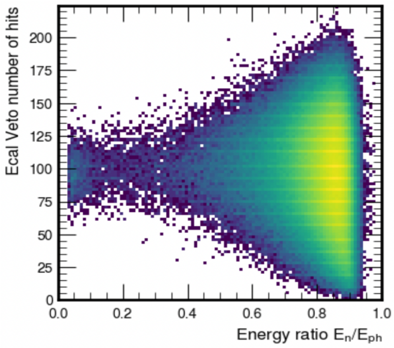

(a) Number of hits in the ECal.

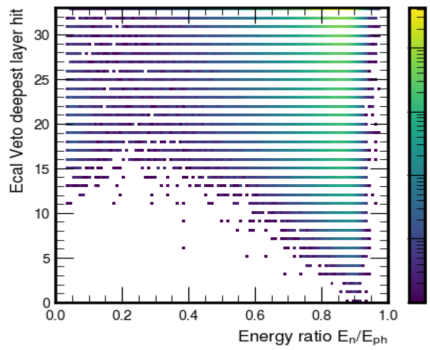

(b) Deepest layer with hits in the ECal.

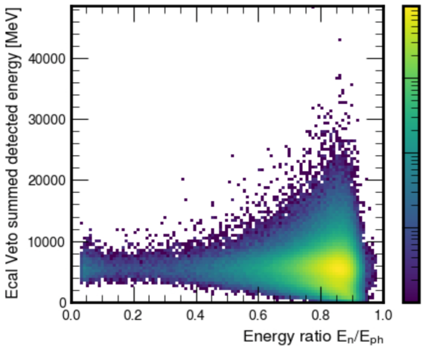

(c) Total reconstructed energy in the ECal.

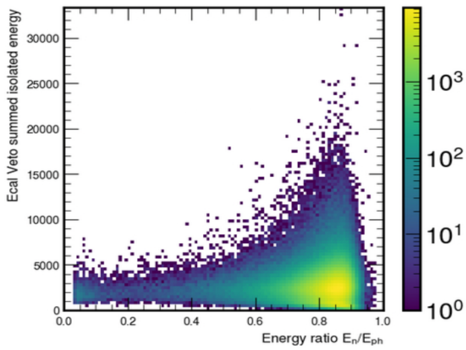

(d) Total energy from isolated hits in the ECal.

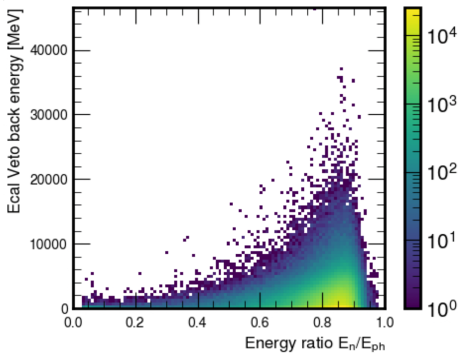

(e) Total energy near the back of the ECal.

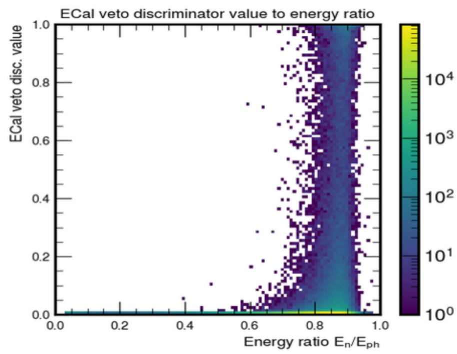

(f) Discriminator value.

Figure 4.2: Distributions of a handful of ECal Veto parameters against the neutron-photon energy ratio for 10^6 events.

Events with discriminator value > 0.2 constitute 10799, or about 1.1%, of the original 10^6 events. Whether or not this is sufficient for calibration will be discussed later. As the photo-nuclear events we are looking at are very DM signal-like to the ECal Veto, it should come as no surprise that the discriminator value is the best option to select events where the neutron retains most of the photon energy. These events form a much narrower linear relationship between neutron kinetic energy and photon energy, see Fig. 4.3. To better compare the effect of this veto variable cut, a histogram of the neutron-photon energy ratio can be found in Fig. 4.4. The average energy ratio for the full dataset is ~ 0.82, with a standard deviation of ~ 0.074. Meanwhile, for the cut events, their average energy ratio is ~ 0.87 with a standard deviation of ~ 0.034, or less than half that of the full dataset. These cut events will be used for the remainder of the thesis.

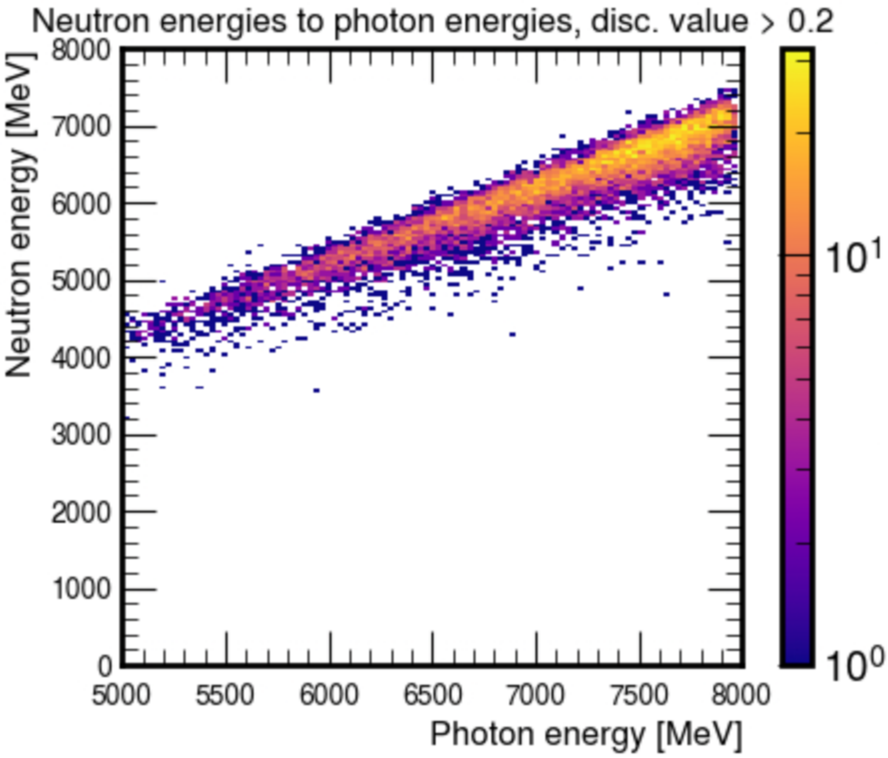

Figure 4.3: The relation between simulated neutron energy and simulated photon energy, filtered for events with ECal Veto discriminator value > 0.2.

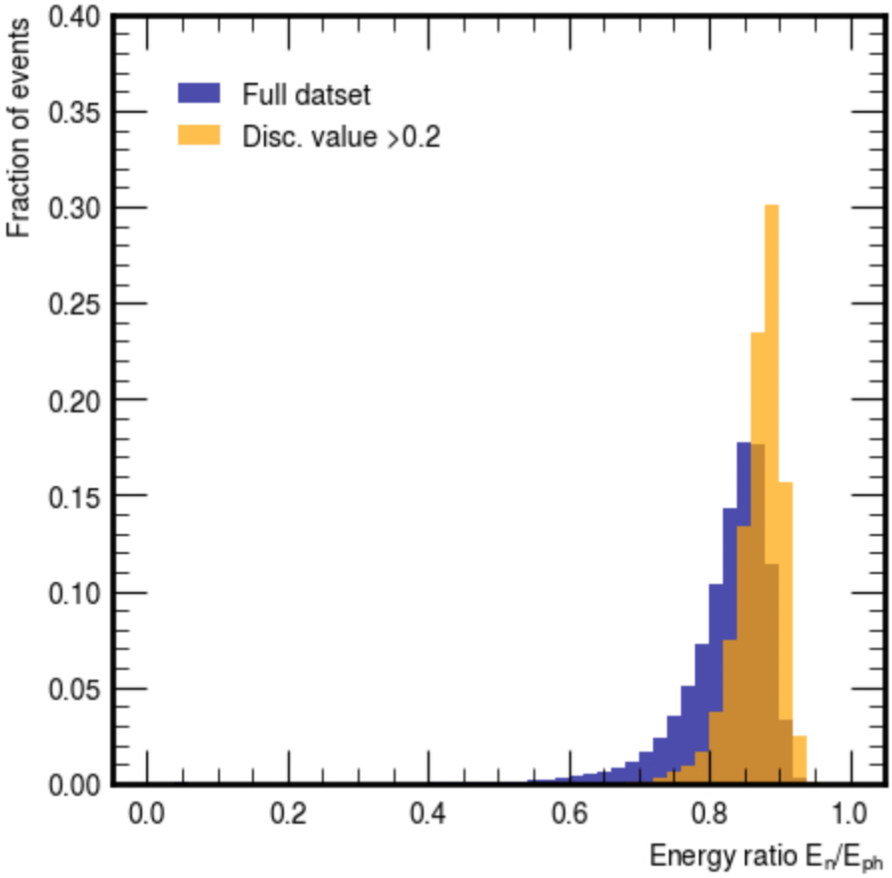

Figure 4.4: Histograms of neutron-photon energy ratios. The blue histogram is full dataset while the yellow histogram is for events with ECal Veto discriminator value > 0.2. Note that both histograms are normalized to their own dataset.

4.2 Detector Response

As we wish to see how well the detectors respond to the simulated particles, we plot their total measured energies against the simulated neutron energy. First we compare the weighted simulated ECal energy to the reconstructed one, see Fig. 4.5. Their distribution is almost identical, but differ by a factor 1.6 in total ECal energy. This may be due to additional steps in the conversion from digital signal to reconstructed signal that were not accounted for. Whatever the case, the reconstructed energy is the most true-to-life and provides the more representative ECal response. There is the occasional odd event that is reconstructed with *more* than 8 GeV energy, and many more in the whole dataset. From the stochastic nature of particle-detector interactions, one could expect some smearing of detected energy above what is physically possible. In the full dataset, there were several events that were reconstructed with over 20 GeV, see Fig. 4.2, which is extraordinary for smearing. At an internal LDMX meeting it was clarified that these events had contributions from light ions and light nuclei generated in background processes in the simulation. These are basically ”nuclear shrapnel” from hadronic interactions that rarely deposit their energy in the ECal; although when they do, they deposit a lot of energy. The ECal is not calibrated with these in mind, so their energies are overestimated by the weighted layers in the ECal. Fortunately, they are few and far between and of no concern for this thesis.

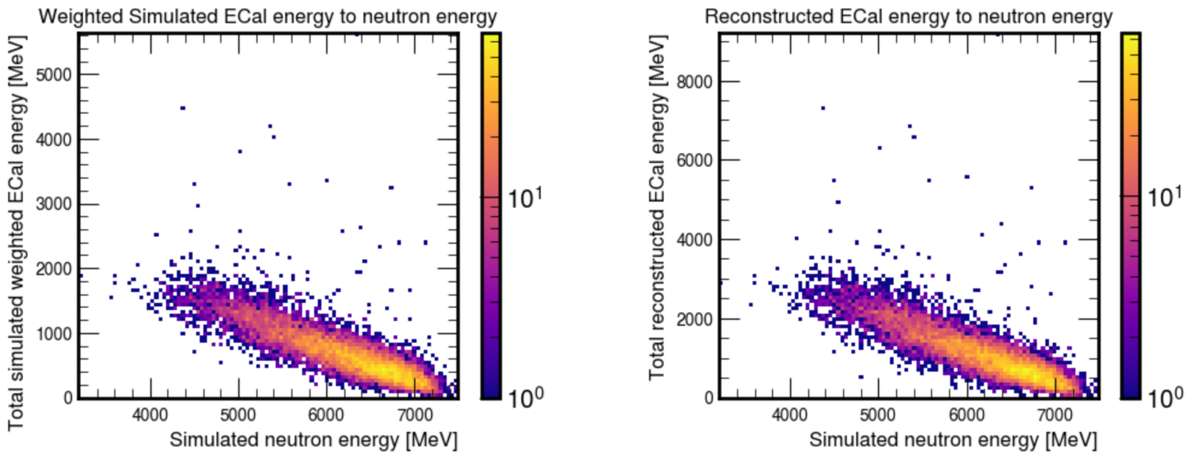

(a) Simulated weighted ECal energy measurements versus simulated neutron energy.

(b) Reconstructed ECal energy measurements versus simulated neutron energy.

Figure 4.5: Simulated weighted energy and reconstructed total energy for the ECal versus simulated neutron energy.

The HCal has a more broadened response to the simulated neutron, see Fig. 4.6. The simulated and reconstructed energies in the HCal are fairly close, but neither reflect the “true” simulated neutron energy. Naturally, this is because the HCal has not been calibrated and its layers not assigned scaling weights. The reconstructed energy merely shows what its readout electronics yield, it does not yet take into account the absorbing layers between the measurement layers.

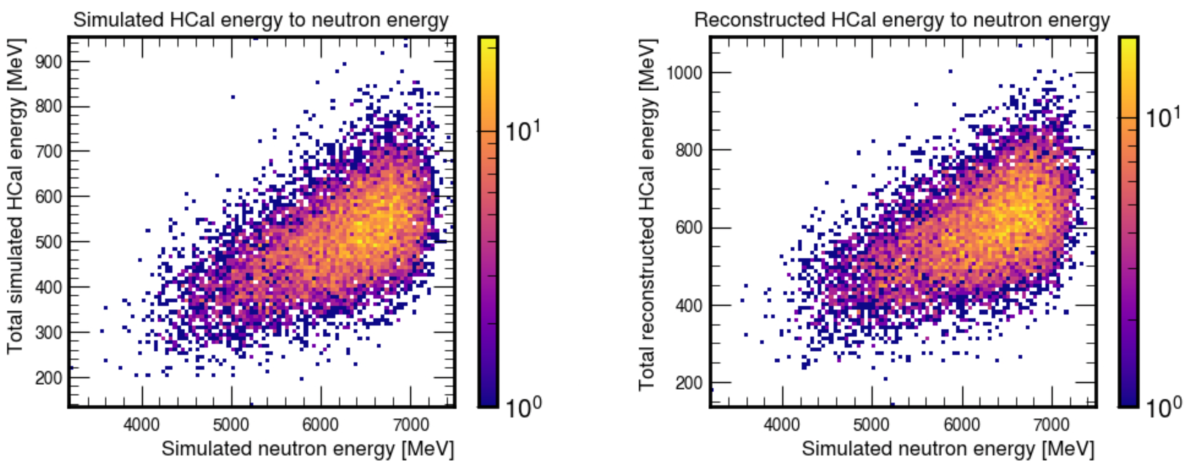

(a) Simulated HCal energy depositions versus simulated neutron energy.

(b) Reconstructed HCal energy measurements versus simulated neutron energy.

Figure 4.6: Simulated and reconstructed total energy for the HCal versus simulated neutron energy.

Before we calculate any linear relationships between the detector responses and simulated neutron energy, we should transform the ECal response to something more akin to missing electron energy. As all of the electron’s remaining energy is captured in the ECal, this is as simple as letting the missing energy be equal to the initial energy (which is always 8 GeV) minus the total reconstructed ECal energy. This, however, is the energy we expect to find in the photon from the bremsstrahlung interaction. To best compare it to the neutron energy, we must reduce it to the same fraction of energy that the neutron retains. For the veto cut events, this was 0.872 as mentioned in Section 4.1. Now we have what we might call “expected neutron energy”. If we let E_e be the initial electron energy, E_{ECal} be the reconstructed ECal energy, E_{ph} be the photon energy, $E_{n,sim}$ be the simulated neutron energy and $E_{n,exp}$ be the expected neutron energy, we can write their relation as

$$E_{n,exp} = (E_e - E_{ECal}) \cdot mean\left(\frac{E_{n,sim}}{E_{ph}}\right). \tag{4.1}$$

First, we want to find a linear relation between the expected neutron energy $E_{n,exp}$ and the simulated neutron energy $E_{n,sim}$. To compensate for the energy distributions and outliers, we first histogram the expected neutron energy into 200 MeV bins between 3977-6977 MeV. The upper bound of this range is $8000 \cdot 0.872 \approx 6977$ MeV, the maximum expected neutron energy based on missing electron energy. The lower bound is 3000 MeV below this, below which the data became too sparse for our purposes. Within each of these bins, the simulated neutron data was histogrammed and a Gaussian function was fit to their distribution. A linear fit was finally taken between the means of these Gaussian fits and the midpoint of the expected neutron energy bins. The linear equation becomes

$$E_{n,sim} = -612 + 1.125 \cdot E_{n,exp} \text{ [MeV]} \tag{4.2}$$

and can be seen in Fig. 4.7a. The linear coefficient being larger than 1 tells us that the expected neutron energy underestimates the neutron energy on average, possibly due to the asymmetric distribution of the neutron-photon energy ratio.

Similarly, for the HCal, we want to find a linear relation between the simulated neutron energy $E_{n,sim}$ and the reconstructed HCal energy E_{HCal}. This is the other way around than for the ECal, so for this we first histogram the simulated neutron energy into 200 MeV bins between $3900 - 7500$ MeV. Within each bin, the HCal energies are histogrammed and a Gaussian function is fit to the data. A linear fit was finally taken between the means of these Gaussian fits and the midpoints of the simulated neutron energy bins. The linear equation was

$$E_{HCal} = 52.7 + 0.0864 \cdot E_{n,sim} \text{ [MeV]} \tag{4.3}$$

and can be seen i Fig. 4.7b. The reciprocal of the linear coefficient gives us an estimate of the statistical weight the HCal needs to match the simulated energies. This reciprocal is ~ 12 and is on the same order of magnitude as those for the ECal.

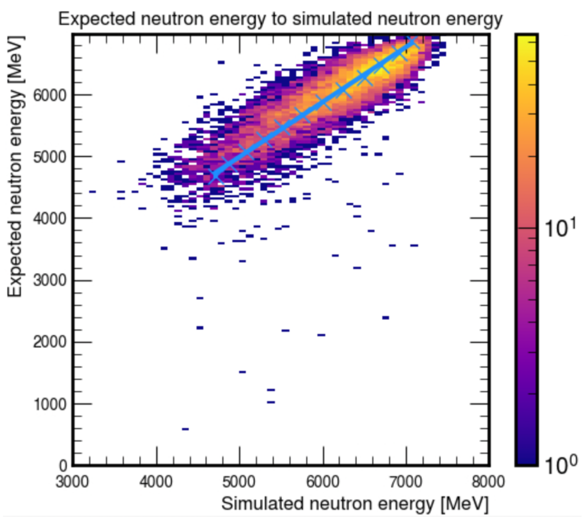

(a) Expected neutron energy versus simulated neutron energy.

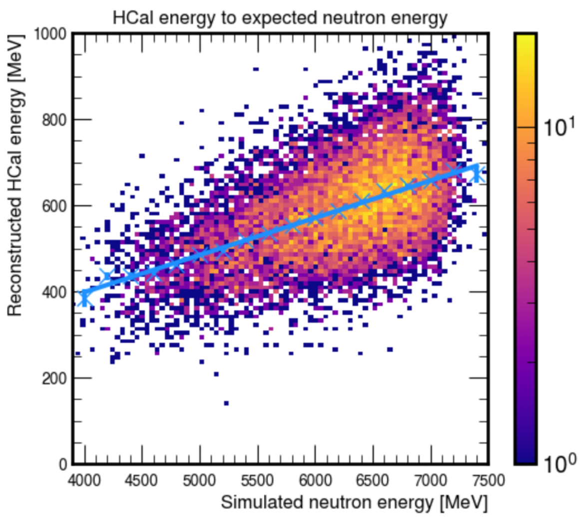

(b) Reconstructed HCal energy measurements versus simulated neutron energy.

Figure 4.7: Reconstructed total energy for the ECal and HCal versus simulated neutron energy.

Due to the wide distribution of HCal measurements for a given neutron energy, there is some concern that the HCal will not be able to properly resolve the energy very well. We estimated the relative resolution R (within each neutron energy bin) as the standard deviation of the HCal energy σ_{HCal} divided by the mean HCal energy $\bar{E}_{HCal}$ (both taken from the Gaussian fit). That is to say:

$$R = \frac{\sigma_{HCal}}{\bar{E}_{HCal}} \tag{4.4}$$

The errors of these estimates ΔR are based on the errors and covariance of the parameters from the Gaussian fits, $\Delta\bar{E}_{HCal}$, $\Delta\sigma_{HCal}$ and $C(\sigma_{HCal}, \bar{E}_{HCal})$, and is approximated to first order by

$$\Delta R \approx R\sqrt{\left(\frac{\Delta\sigma_{HCal}}{\sigma_{HCal}}\right)^2 + \left(\frac{\Delta\bar{E}_{HCal}}{\bar{E}_{HCal}}\right)^2 - 2\frac{C(\sigma_{HCal}, \bar{E}_{HCal})}{\sigma_{HCal}\cdot\bar{E}_{HCal}}}. \tag{4.5}$$

The relative resolution is expected to fall as one over the square root of the particle energy [12], in this case neutron energy, so

$$R \propto E_{n,sim}^{-0.5}. \tag{4.6}$$

Fitting a monomial function to the relative resolutions between neutron energies of $3900 - 7500$ MeV resulted in a fall as

$$R = 1.49 \cdot E_{n,sim}^{-0.250} \tag{4.7}$$

when measured in MeV, see Fig. 4.8. This does not quite match up to theory, although the fit admits to very large errors in the estimated parameters. The amplitude is returned as 1.49 ± 1.34 and the exponent as -0.250 ± 0.103. With uncertainties of this size, the fit gives little information on the quality of the resolution. We consider instead the actual values of the resolution. From internal communications [19], we expect the HCal resolution to be approximately

$$R \approx 15.8 \cdot E_n^{-0.5} \tag{4.8}$$

for energies around 1000 MeV, again measured in MeV (this yields a resolution around $R = 0.5$ for 1 GeV particles). Extrapolating this formula for 4000 MeV and 7000 MeV yield $R = 0.25$ and $R = 0.189$ respectively, which is close to the values in Fig. 4.8.

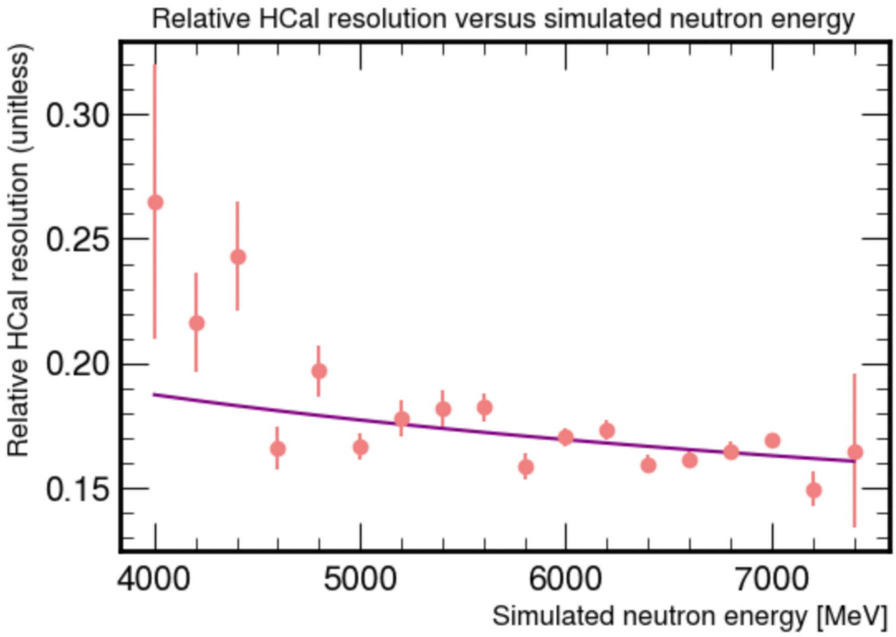

Figure 4.8: Relative resolution of reconstructed HCal energy within neutron energy bins of 200 MeV. In purple is an attempted monomial fit.

4.3 Direct ECal to HCal Comparison

The real experiment will not have the possibility of comparing the detector responses to the exact neutron energies. It will have to directly compare the HCal measurements to the ECal measurements and convert them to an expected neutron energy. By combining the linear formulae 4.2 and 4.3, we find

$$E_{HCal} = -0.177 + 0.0972 \cdot E_{n,exp} \text{ [MeV]}. \tag{4.9}$$

If we plot the reconstructed HCal energy against the expected neutron energy and apply the same treatment we did against the simulated neutron energy, we get the linear relation

$$E_{HCal} = 2.65 + 0.0965 \cdot E_{n,exp} \text{ [MeV]}, \tag{4.10}$$

which is similar to that of equation 4.9, see Fig. 4.9.

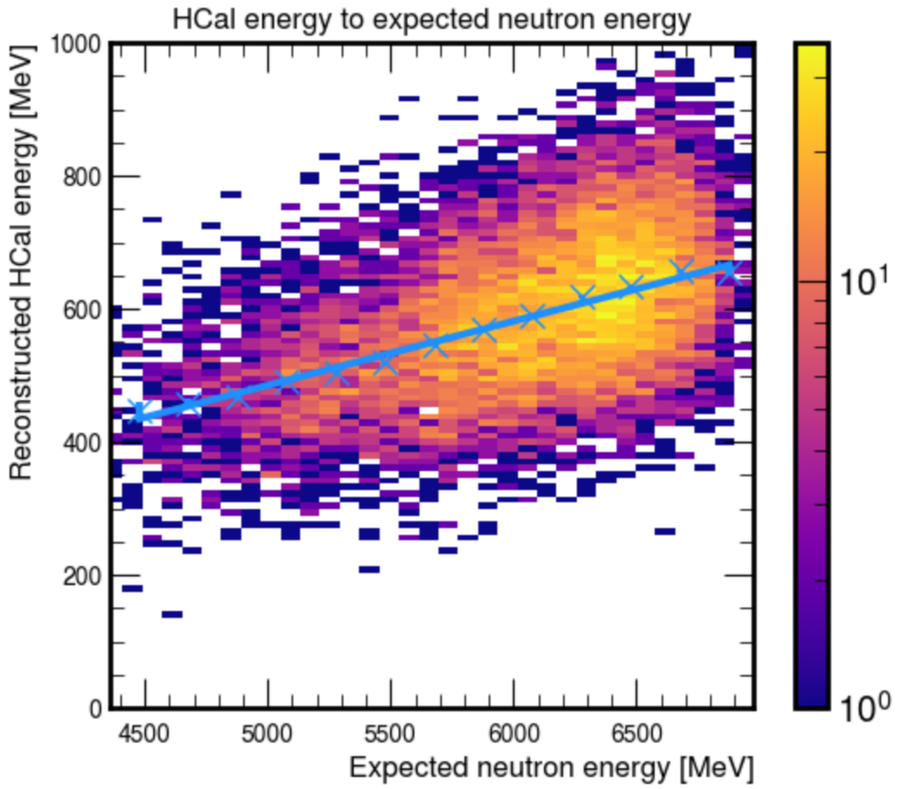

Figure 4.9: Reconstructed HCal energy versus expected neutron energy.

The 10,799 events that were passably discriminated by the ECal veto algorithm had similar distributions of neutron-photon energy ratios and detector responses across the entire span of discriminator values between $0.2 - 1.0$. They did not, however, provide sufficient samples for HCal calibration across the entire energy span between $0 - 8$ GeV. As the neutrons originated from photons within the energy range $5 - 8$ GeV, we anticipated a similar subset of the whole energy span could be calibrated; or perhaps a shifted subset due to the neutron-photon energy ratio being less than 1. The most promising such range is most likely neutron energies between $4.5 - 7.5$ GeV, with a near-theoretical relative energy resolution and decent sample size. If the HCal response can be interpolated linearly, single-neutron photo-nuclear events could at least contribute to the calibration of the HCal.

4.4 Outlook

We have only simulated events with photon energies above 5 GeV because the real experiment will ignore events with less than 5 GeV missing electron energy. The estimate of 10^6 single-neutron photo-nuclear events from Section 2.2.4 does take this into account, so the sample size in this simulation is a good representative of real data. What was not taken into account, however, was the nuclear binding energies of the nuclei involved in the photo-nuclear interactions, nor the distribution of nuclei. These nuclei are impossible to discern in the real experiment, but future simulations could account for them to provide more representative data. Their effect on the simulation would be to cause slightly more variance in the neutron energies, causing a slightly poorer resolution of the HCal energies. The distribution of initial electron energies were also unaccounted for, and these will actually be measurable in the real experiment thanks to the trackers. Including this would likewise provide more representative data. The inittal electron energy distribution is very narrow and would only have a marginal effect on the variance in missing electron energy and/or photon energy. Additionally, we have made no attempt to assign statistical weights to the layers in the HCal as it was out of the scope of this project. While the real detectors must be calibrated independently of simulations, having an idea of the size and distribution of weights, particularly relative to the ECal, from simulations could help provide a starting point. Other background processes are also worth investigating to aid calibrating the HCal. Particularly neutral kaons, which occur at around the same relative rate as single neutrons, may provide similar results as those found in this project. Based on the results of previous LDMX research, simulations with other frameworks, such as FLUKA, would also be useful to double check the viability of using single-neutron photo-nuclear events for LDMX HCal calibration.

Chapter 5

Conclusion

In this thesis we have simulated 10^6 single-neutron photo-nuclear events for the (upcoming) Light Dark Matter eXperiment and investigated the feasibility of calibrating the LDMX HCal with them. We have found that the fraction of these events that the ECal BDT assigns a discriminator value above 0.2 shows the lowest variance ratio between the neutron energy and the photon energy. The neutron energies of these events also show linear relations with the detector responses. Additionally, the relative energy resolution in the HCal showed promising values close to theory, although the theoretical resolution-to-energy relation could not be established. The direct comparison between ECal and HCal also showed a well-defined linear relation with adequate amounts of data between neutron energies of $4.5 - 7.5$ GeV. If single-neutron photo-nuclear events can be distinguished at the real experiment, we believe they can contribute well to the calibration of the HCal.

Bibliography

[1] Salucci P. The distribution of dark matter in galaxies. The Astronomy and Astrophysics Review. 2019 February;Volume 27. Accessed 2025-04-24. Available from: https://doi.org/10.1007/s00159-018-0113-1.

[2] Åkesson, T, Berlin, A, Blinov, N et al. Light Dark Matter eXperiment (LDMX). 2018 August. Accessd 2025-04-24. Available from: https://arxiv.org/pdf/1808.05219.pdf.

[3] Stanford University. SLAC National Accelerator Laboratory. Accessed 2025-06-06. Available from: https://www6.slac.stanford.edu.

[4] CERN. Geant4. Accessed 2025-06-06. Available from: https://geant4.web.cern.ch.

[5] Bertone, G & Hooper, D. A History of Dark Matter. Reviews of Modern Physics. 2018 October;Volume 90. Accessed 2025-04-29. Available from: https://arxiv.org/pdf/1605.04909.

[6] Curtin D. MODEL BUIDING AND COLLIDER PHYSICS ABOVE THE WEAK SCALE. Cornell University. 2011 August. Accessed 2025-04-24. Available from: https://www.classe.cornell.edu/rsrc/Home/Research/GradTheses/Curtin_David.pdf.

[7] Buchmueller, O, Cavanaugh, R, De Roeck, A et al . Likelihood Functions for Supersymmetric Observables in Frequentist Analyses of the CMSSM and NUHM1. The European Physics Journal C. 2009 October;Volume 64. Accessd 2025-04-30. Available from: https://arxiv.org/pdf/0907.5568.

[8] Wilczek F. Time's (Almost) Reversible Arrow. Quanta Magazine. 2016 January. Accessed 2025-04-30. Available from: https://www.quantamagazine.org/how-axions-may-explain-times-arrow-20160107/.

[9] Weinberg S. A New Light Boson? Physical Review Letters. 1978 January;Volume 40. Accessed 2025-04-30. Available from: https://web.archive.org/web/20190224041317/http://pdfs.semanticscholar.org/5063/f691a0b3fe1e0e6c3fc890c1f67e714ebb6d.pdf.

[10] De Luzio, L, Giannotti, M, Nardi, E & Visinelli, L . The landscape of QCD axion models. Physics Reports. 2020 July;870. Accessed 2025-04-30. Available from: https://arxiv.org/pdf/2003.01100.

[11] Brown, R M & Cockerill, D J A . Electromagnetic Calorimetry. Nuclear Instruments and Methods in Physics Research A. 2012 February;Volume 666. Accessed 2025-05-01. Available from: https://www.sciencedirect.com/science/article/pii/S0168900211005572.

[12] Akchurin, N & Wigmans, R . Hadron Calorimetry. Nuclear Instruments and Methods in Physics Research A. 2012 February;Volume 666. Accessed 2025-05-01. Available from: https://www.sciencedirect.com/science/article/pii/S0168900211019851.

[13] The LDMX Collaboration. Photon-rejection power of the Light Dark Matter eXperiment in an 8 GeV beam; 2023. Accessed 2025-05-19. Available from: https://link.springer.com/article/10.1007/JHEP12(2023)092.

[14] FLUKA team. FLUKA. Accessed 2025-06-06. Available from: http://www.fluka.org/fluka.php?

[15] Elén, E & Sarmiento, L G . Private communication. 2025 February.

[16] The LDMX Collaboration. ldmx-sw. Accessed 2025-05-05. Available from: https://github.com/LDMX-Software/ldmx-sw/tree/trunk.

[17] The LDMX Collaboration. LU-student-projects. Accessed 2025-05-22. Available from: https://github.com/bryngemark/LU-student-projects/tree/main.

[18] The LDMX Collaboration. LDMX Software. Accessed 2025-05-17. Available from: https://ldmx-software.github.io/index.html.

[19] Pöttgen R. Private communication. 2025 May.

Appendix A

Simulated Hits to Reconstructed Hits

The conversion from simulated energy deposition in a detector to reconstructed energy measurement is not quite as simple as just multiplying the energy deposition by a statistical weights. The calculations in the code are based on minimally ionizing particles (MIPs), essentially the minimum possible signals that can be measured. The electrical signal from an energy deposition is, in the reconstruction, converted into an equivalent number of MIPs, N_{MIP}, that would have created an identical signal. This, together with the constant energy per MIP $E_{MIP} = 0.13$ MeV, is used to calculate the reconstructed energy deposition

$$E_{dep} = N_{MIP} \cdot E_{MIP}.$$

Finally, the statistical weight of layer i, w_i, and a constant (second order) energy correction factor $C_2 \approx 1.015$ is used to calculate the final reconstructed energy measurement

$$E_{rec} = (N_{MIP} \cdot w_i + E_{dep}) \cdot C_2.$$